HETEROCYCLES, Vol. 75, No. 9, 2008, pp. 2187 - 2192. © The Japan Institute of Heterocyclic Chemistry
Received, 7th April, 2008, Accepted, 12th May, 2008, Published online, 15th May, 2008. COM-08-11407

PEROXISOME PROLIFERATOR-ACTIVATED RECEPTOR (PPAR) AGONISTS WITH 3,4-DIHYDRO-2*H*-BENZO[*e*][1,3]OXAZINE AND 2,3,4,5-TETRAHYDROBENZO[*f*][1,4]OXAZEPINE SKELETONS: EFFECTS OF CYCLIZATION OF LINKER MOIETY ON PPAR-AGONISTIC ACTIVITY

Kenji Ohgane,[a] Jyun-ichi Kasuga,[a] Takuji Ohyama,[b] Yuko Hirakawa,[b] Kosuke Morikawa,[b] Makoto Makishima,[c] Yuichi Hashimoto,[a] and Hiroyuki Miyachi[a,*]

[a] Institute of Molecular and Cellular Biosciences, University of Tokyo. Yayoi, Bunkyo-ku, Tokyo 113-0032, Japan. [b] The Takara-Bio Endowed Division, Institute for Protein Research, Osaka University, 6-2-3, Furuedai, Suita, Osaka 565-0874, Japan. [c] Nihon University School of Medicine, 30-1 Oyaguchi-kamicho, Itabashi-ku, Tokyo 173-8610, Japan.

Abstract – Conformationally restricted heterocyclic derivatives of KCL ((*S*)-2-{4-methoxy-3-[4-(trifluoromethyl)benzylcarbamoyl]benzyl}butanoic acid), which exhibit selective PPARα-agonistic activity, were prepared to examine the significance of the amide bond of KCL. *In vitro* transactivation assay clearly indicated that introduction of a 2-position fluorine atom enhanced PPARs-agonistic activity as expected, while cyclization of the amide bond caused a drastic decrease of PPARs-agonistic activity.

The PPARs are ligand-dependent transcription factors belonging to the nuclear receptor superfamily; they are activated by endogenous fatty acids and their metabolites, and by synthetic ligands.[1] Three subtypes have been isolated to date: PPARα, PPARδ and PPARγ. These subtypes share a high level of structural homology, but each has distinct physiological functions and shows a unique tissue distribution pattern. PPARα is expressed mostly in tissues involved in lipid oxidation, such as liver, kidney, skeletal and cardiac muscle and adrenal glands. PPARγ is expressed in adipose tissue, macrophages and vascular smooth muscles. In contrast to the specific distributions of PPARα and PPARγ, PPARδ is ubiquitously expressed.[2] Upon endogenous and/or synthetic agonist binding, PPARs heterodimerize with another nuclear receptor

partner, retinoid X receptor (RXR), and the heterodimers regulate gene(s) expression by binding to specific consensus DNA sequences, termed peroxisome proliferator responsive element (PPRE). These elements are a direct repeat of the hexameric AGGTCA recognition motif, separated by one nucleotide (DR1), present in the promoter region of the target genes.[3]

PPARα regulates genes involved in fatty acid uptake, β-oxidation, and ω-oxidation. It down-regulates apolipoprotein C-III, and it also regulates genes involved in reverse cholesterol transport, such as apolipoprotein A-I and apolipoprotein A-II.[4] Therefore, PPARα agonists are candidate therapeutic agents for disorders of lipid and lipoprotein homeostasis.

Previously, we have designed and synthesized a series of substituted phenylpropanoic acid human PPARα-selective agonists, exemplified by KCL (Figure 1).[5-8] Here, we present further structural development studies designed to identify structure-activity relationships of phenylpropanoic acid-type PPARα-selective agonists. In order to confirm the recent finding that the introduction of fluorine at the 2-position enhanced PPARs-agonistic activity,[9] and to examine the significance of the 2-methoxybenzamide part of KCL, we planned to prepare 2-fluorinated KCL (KCL-F), and cyclic analogs of KCL-F, i.e., propanoic acids with 3,4-dihydro-2*H*-benzo[*e*][1,3]oxazine or 2,3,4,5-tetrahydrobenzo[*f*][1,4]oxazepine structure (Figure 1).

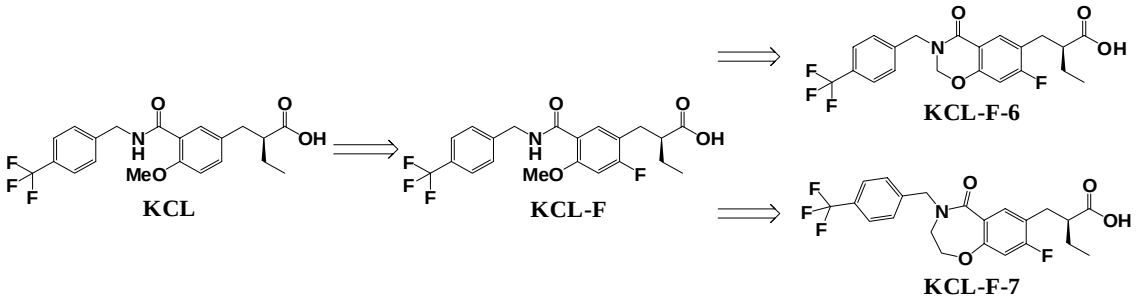

Figure 1. Structural development of PPARα-selective agonist KCL

The synthetic routes to the target compounds are depicted in Scheme 1. 2-Fluoro-4-methoxybenzaldehyde (**1**) was treated with (*S*)-*N*-butyryl-4-benzyloxazolidin-2-one under Evans's asymmetric aldol condensation conditions,[10] and subsequent dehydroxylation afforded the optically active oxazolidin-2-one derivative (**2**) in 78% yield (two steps). The chiral auxiliary was replaced with ethyl ester by using $Ti(OEt)_4$ to afford the ethyl propionate derivative (**3**) in 56% yield. Compound (**3**) was formylated with $CHCl_2OMe/TiCl_4$ in CH_2Cl_2 (yield 80%), and then Kraus oxidation[11] (yield 98%), followed by amidation with 4-(trifluoromethyl)benzylamine afforded the key intermediate (**6**) (yield 45%). Compound **6** was hydrolyzed under acidic conditions to afford the desired compound, **KCL-F** (yield 38%). Demethylation

of compound **6** with BBr_3 in CH_2Cl_2 afforded phenol derivative **7** in 91% yield, and this was treated with trioxane under acidic conditions (yield 96%), followed by acidic hydrolysis to afford the 3,4-dihydro-2*H*-benzo[*e*][1,3]oxazine derivative, **KCL-F-6**, in 49% yield. When **7** was treated with 1,2-dibromoethane in the presence of K_2CO_3 in CH_3CN, we obtained only *o*-alkylated compound (**9**) in 43% yield. Therefore, the amide of **9** was deprotonated with LiHMDS in DMF to afford the desired cyclic derivative of the 2,3,4,5-tetrahydrobenzo[*f*][1,4]oxazepine derivative (**10**) in 77% yield. This was hydrolyzed to afford **KCL-F-7** in 49% yield.[12] The optical purity of all the synthesized products was determined to be >98% e.e. with HPLC analysis using chiral support.

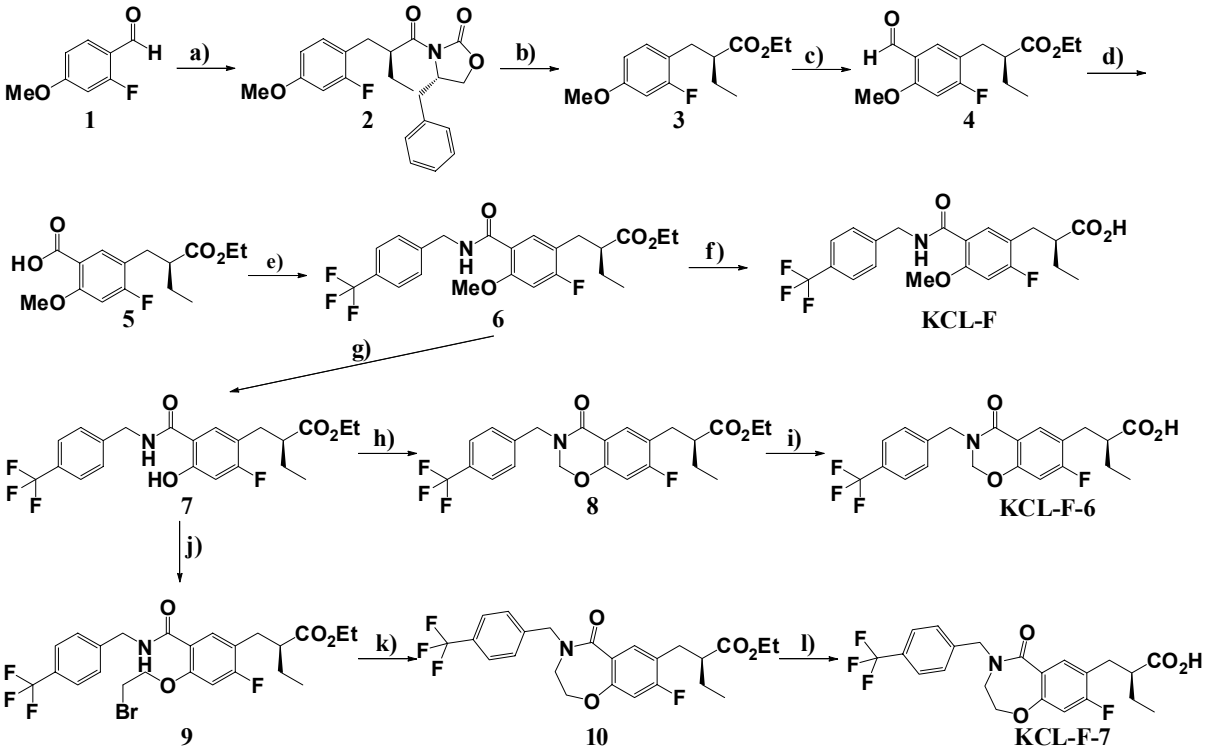

Scheme. 1. Synthetic routes to KCL derivatives
Reagents and conditions; a) 1) (*S*)-4-benzyl-*N*-butyryloxazolidin-2-one, Bu_2BOTf, triethylamine, CH_2Cl_2, -78-0ºC, 2) $(Et)_3SiH$, CH_2Cl_2, rt, 78% (two steps). b) $Ti(OEt)_4$, EtOH, 80ºC, 56%. c) $CHCl_2OMe$, $TiCl_4$, CH_2Cl_2, -78ºC –rt., 80%. d) 2-methyl-2-butene, $NaClO_2$, aq$NaHPO_4$, *t*BuOH, rt. 98%. e) EDCI, HOBt, triethylamine, CH_2Cl_2, rt, 45%. f) HCl, 1,4-dioxane, 80ºC, 38%. g) BBr_3, CH_2Cl_2, -78ºC, 91%. h) trioxane, HCl, AcOH, AcOEt, 80ºC, 96%. i) HCl, 1,4-dioxane, 80ºC, 49%. j) 1,2-dibromoethane, K_2CO_3, CH_3CN, reflux, 43%. k) LiHMDS, DMF, 0ºC, 77%. l) HCl, 1,4-dioxane, 80ºC, 49%.

In vitro transactivation activities of the present series of compounds along with the positive control KCL are summarized in Table 1. Introduction of fluorine at the 2-position enhanced PPARs-agonistic activity as expected. KCL-F exhibited more potent PPARs-agonistic activity than KCL for every PPAR subtype. The effect was most marked in the case of PPARα, i.e., KCL-F exhibited 10 times greater activity than the positive control, KCL.

Table 1. In vitro transactivation assay of the present series of compounds as LXR ligands.

Compd.	Structure	EC_{50} (nM)[a]		
		PPARα	PPARδ	PPARγ
KCL	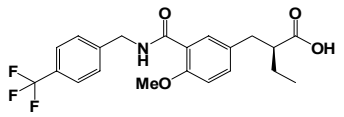	13.2±1.94	121±6.6	1411±438
KCL-F	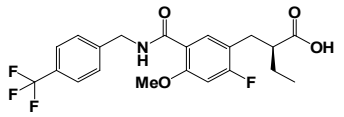	1.69±0.69	66.0±8.3	835±130
KCL-F-6	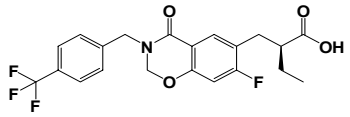	918±65	2270±620	2920±110
KCL-F-7	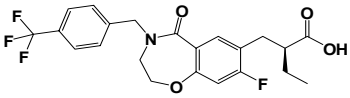	241±38	525±10	3320±88

a) Compounds were screened for agonist activity on LXR-GAL4 chimeric receptors in transiently transfected HEK-293 cells. EC_{50} value is the molar concentration of the test compound that affords 50% of the maximal reporter activity.

Although the reason why fluorine substitution at the 2-position enhanced PPARα activity so effectively is uncertain, a recent X-ray crystallographic analysis of the complex of TIPP-401 ((*S*)-2-(3-{[2-fluoro-4-(trifluoromethyl)benzamido]methyl}-4-methoxybenzyl)butanoic acid), a structurally related PPARα/δ dual agonist with a common α-ethyl-(4-methoxyphenyl)propanoic acid framework, with human PPARδ (Figure 2) indicated that the central benzene ring was positioned in the middle of the Y-shaped binding pocket, surrounded by the hydrophobic amino acids Cys285, Phe327, Ile363, Ile364, Lys367, and Met453 (The Protein Data Bank code for the PPARδ/TIPP-401 complex is 2ZNQ). The 2-position hydrogen atom of TIPP-401 faced a small dimple, composed of Ile363, Ile364, and Lys367 (Figure 2(B)). The corresponding amino acids forming the dimple are Ile354, Met355, and Lys358 in the case of PPARα, and Phe363, Met364, and Lys367 in the case of PPARγ . We speculate that the introduced 2-fluorine substituent influences van der Waals interaction and/or hydrophobic interaction with the dimple region most effectively in the case of the PPARα subtype. On the other hand, cyclization of the amide portion of KCL to form 3,4-dihydro-2*H*-benzo[*e*][1,3]oxazine (KCL-F-6) or 2,3,4,5-tetrahydrobenzo[*f*][1,4]oxazepine (KCL-F-7) greatly decreased PPARs-agonistic activity and PPAR subtype-selectivity, especially in the case of KCL-F-6.

This means that the presence of 2-methoxybenzamide structure is crucially important for potent and subtype-selective PPARα activation. In the TIPP-401 - PPARδ LBD complex, the methyl moiety of the 4-position methoxy group has a hydrophobic interaction with the binding pocket surrounded by Leu330,

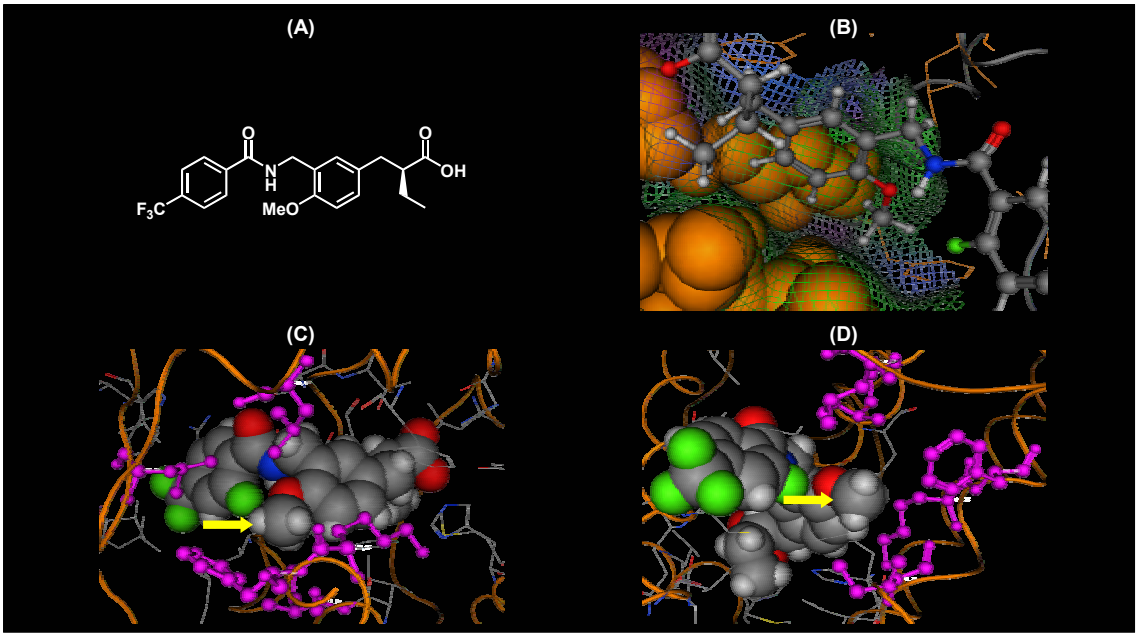

Figure. 2. Three-dimensional structure of TIPP-401 complexed with human PPARδ ligand binding domain (LBD). (A) Chemical structure of TIPP-401. (B) Zoomed view of the complex. TIPP-401 is represented as a "ball and stick" model. The amino acids interacted with the center benzene ring are colored orange. (C) Zoomed front view of the complex. TIPP-401 is represented by a "space filling" model. The amino acids that interact with the methoxy group of TIPP-401 are colored pink. The yellow arrow indicates the position of the methoxy group. (D) Zoomed side view of the complex. TIPP-401 is represented by a "space filling" model. The amino acids that interact with the methoxy group of TIPP-401 are colored pink. The yellow arrow indicates the position of the methoxy group

Leu339, Ile364, Lys367, and Phe368 (Figure 2 (C, D)). This pocket is well conserved among all PPAR subtypes (Leu321, Met330, Met355, Lys358, and Phe359 in the case of PPARα, and Leu330, Val339, Met364, Lys367, and Phe368 in the case of PPARγ).

The decrease in PPAR activity of KCL-F-6 and KCL-F-7 might be attributed partly to the lack of this hydrophobic interaction as a result of linking the methoxy group and the amide portion. Furthermore, conformational restriction might result in a conformation unfavorable for binding to the Y-shaped binding pocket of PPARs. This might be one reason why the 6-6-fused 3,4-dihydro-2*H*-benzo[*e*][1,3]oxazine (**KCL-F-6**) exhibited weaker PPARs-agonistic activities than the 6-7-fused 2,3,4,5-tetrahydrobenzo[*f*][1,4]oxazepine (**KCL-F-7**).

In conclusion, we have developed 2-fluorinated KCL (KCL-F), and cyclic analogs of KCL-F, i.e., 3,4-dihydro-2*H*-benzo[*e*][1,3]oxazine-type KCL (**KCL-F-6**) and 2,3,4,5-tetrahydrobenzo[*f*][1,4]-oxazepine-type KCL (**KCL-F-7**), and found that the introduction of fluorine at the 2-position enhanced all PPAR-agonistic activities, while cyclization of the amide portion of KCL greatly decreased all PPAR-agonistic activities, as well as the PPAR subtype selectivity. Further three-dimensional structure-activity relationship studies with the aid of X ray crystallographic analysis are on-going.

ACKNOWLEDGEMENTS

The work described in this paper was partially supported by a Grant-in-aid for Scientific Research from The

Ministry of Education, Culture, Sports, Science and Technology, Japan, and by a grant from Keimeikai Foundation.

REFERENCES AND NOTES

1. P. T. Meinke, H. B. Wood, and J. W. Szewczyk, *Ann. Rep. Med. Chem.,* 2006, **41**, 99.
2. T. M. Willson, P. J. Brown, and D. D. Sternbach, *J. Med. Chem.*, 2000, **43**, 527.
3. H. Keller, C. Dreyer, J. Medin, A. Mahfoudi, K. Ozato, and W. Wahli, *Proc. Natl. Acad. Sci.,* 1993, **90**, 2160.
4. B. Staels and J. Auwerx, *Curr. Pharmaceut. Des.,* 1997, **3**, 1.
5. H. Miyachi, M. Nomura, T. Tanase, Y. Takahashi, T. Ide, M. Tsunoda, K. Murakami, K. and K. Awano, *Bioorg. Med. Chem. Lett.,* 2002, **12**, 77.
6. H. Miyachi, M. Nomura, T. Tanase, M. Suzuki, K. Murakami, and K. Awano, *Bioorg. Med. Chem. Lett.,* 2002, **12**, 333.
7. M. Nomura, T. Tanase, and H. Miyachi, *Bioorg. Med. Chem. Lett.,* 2002, **12**, 2101.
8. M. Nomura, T. Tanase, T. Ide, M. Tsunoda, M. Suzuki, H. Uchiki, K. Murakami, and H. Miyachi, *J. Med. Chem.,* 2003, **46**, 3581.
9. J. Kasuga, T. Oyama, Y. Hirakawa, M Makishima, K. Morikawa, Y. Hashimoto, and H. Miyachi, *ChemMedChem*., 2008, submitted.
10. D. A. Evans, J. Bartroli, and T. L. Shih, *J. Am. Chem. Soc*., 1981, **103**, 2127.
11. G. A. Kraus and B. Roth, *J. Org. Chem*., 1980, **45**, 4825.
12. Physicochemical properties of the new compounds are as follows.

    KCL-F ; ^{1}HNMR (500 MHz, $CDCl_3$) δ 8.14 (t, *J* = 5.4 Hz, 1H), 8.11 (d, *J* = 9.0 Hz, 1H), 7.59 (d, *J* =8.5 Hz, 2H), 7.45 (d, *J* =8.5 Hz, 2H), 6.80 (d, *J* = 11.0 Hz, 1H), 4.71 (d, *J* = 5.5 Hz, 2H), 3.92 (s, 3H), 2.93 (dd, *J* = 14.0, 8.5 Hz,1H), 2.86 (dd, *J* = 14.0, 6.5 Hz, 1H), 2.65 (m, 1H), 1.69 (m, 1H), 1.60 (m, 1H), 0.97 (t, *J* = 7.5 Hz, 3H). MS(FAB) 428 $(M+H)^+$. HRMS calcd $(M+H)^+$ 428.1480, found 428.1443. mp 164-166 ºC. $[\alpha]_D^{20}$+ 22.9 (c 0.17, $CHCl_3$).

    KCL-F-6; ^{1}HNMR (500 MHz, $CDCl_3$) δ 7.88 (d, *J* = 8.0 Hz, 1H), 7.62 (d, *J* = 8.0 Hz, 2H), 7.45 (d, *J* = 8.0 Hz, 2H), 7.66 (d, *J* = 11Hz, 1H), 5.14 (s, 1H), 4.79 (s, 1H), 2.94 (dd, *J* = 13.5, 8.5 Hz, 1H), 2.87 (dd, *J* = 13.5, 6.0 Hz, 1H), 1.68 (m, 1H), 1.63 (m, 1H), 0.99 (t, *J* = 7.5 Hz, 3H). MS(FAB) 426 $(M+H)^+$. HRMS calcd $(M+H)^+$ 426.1323, found 426.1346. $[\alpha]_D^{20}$+ 128.3 (c 1.0, $CHCl_3$).

    KCL-F-7; ^{1}HNMR (500 MHz, $CDCl_3$) δ 7.77 (d, *J* = 8.5 Hz, 1H), 7.62 (d, *J* = 8.0 Hz, 2H), 7.46 (d, *J* = 8.0 Hz, 2H), 6.69 (d, *J* =10.5 Hz, 1H), 4.88 (d, *J* = 15.0 Hz, 1H), 4.85 (d, *J* = 15.0 Hz, 1H), 4.21 (m, 2H), 3.50 (m, 2H), 2.90 (m, 2H), 2.65 (m, 1H), 1.69(m, 1H), 1.62 (m, 1H), 0.99 (t, *J* = 7.5 Hz, 3H). MS(FAB) 440 $(M+H)^+$. HRMS calcd $(M+H)^+$ 440.1480, found 440.1507. $[\alpha]_D^{20}$+ 24.2 (c 0.1, $CHCl_3$).